EM Propagation & Atmospheric Effects Assessment

Amalia E. Barrios
SPAWARSYSCEN PACIFIC 5548
Atmospheric Propagation Branch
49170 Propagation Path
San Diego, CA 92152-7385
phone: (619) 553-1429 fax: (619) 553-1417 email: amalia.barrios@navy.mil

Dr. Richard Sprague
SPAWARSYSCEN PACIFIC 5548
Atmospheric Propagation Branch
49170 Propagation Path
San Diego, CA 92152-7385
phone: (619) 553-3064 fax: (619) 553-1417 email: richard.sprague@navy.mil

Award Number: N0001408WX20406
http://areps.spawar.navy.mil/

LONG TERM GOALS

Develop electromagnetic propagation models, that perform equally well over land and sea and in the presence of anomalous propagation conditions for both surface and airborne emitters, for use in operational or engineering propagation assessment systems.

OBJECTIVES

Develop an advanced unified hybrid radio propagation model based on parabolic equation and ray-optics methods for both surface-based and airborne applications. This model is named the Advanced Propagation Model (APM) and is the model used in the Advanced Refractive Effects Prediction System (AREPS). Other objectives are to develop an earth-to-satellite propagation (with METOC) model, ESPM2, suitable for transition to the Advanced Refractive Effects Prediction System (AREPS) and the Naval Integrated Tactical Environmental Subsystem (NITES) 2 Redesign (N2R). The specific technical objectives are to modify the APM to model wideband sources for accurate characterization of the propagation channel for RF communications systems; and modify the ESPM2 to assess the impact on communication system performance of channel limitations imposed by propagation through the ionosphere.

APPROACH

The Joint Tactical Radio System (JTRS) will begin DoD's transition from narrowband (e.g., 5-25 kHz) voice and data point-to-point circuits to networked waveforms such as the WNW, SRW and JAN-TE. The networked waveforms support operating modes with up to 10 MHz bandwidth in normal operation and up to 30 MHz in anti-jam. In the marine environment evaporation and surface based ducts superimpose a complex fading due to multipath, changing the time-averaged mean signal for a given node-to-node path by several dBs. Therefore, the propagation channel must be accurately characterized for wideband

Report Documentation Page

Form Approved
OMB No. 0704-0188

1. REPORT DATE	2. REPORT TYPE	3. DATES COVERED
30 SEP 2008	**Annual**	**00-00-2008 to 00-00-2008**

4. TITLE AND SUBTITLE	5a. CONTRACT NUMBER
EM Propagation & Atmospheric Effects Assessment	5b. GRANT NUMBER
	5c. PROGRAM ELEMENT NUMBER
6. AUTHOR(S)	5d. PROJECT NUMBER
	5e. TASK NUMBER
	5f. WORK UNIT NUMBER
7. PERFORMING ORGANIZATION NAME(S) AND ADDRESS(ES) **SPAWARSYSCEN PACIFIC 5548,Atmospheric Propagation Branch,49170 Propagation Path,San Diego,CA,92152-7385**	8. PERFORMING ORGANIZATION REPORT NUMBER
9. SPONSORING/MONITORING AGENCY NAME(S) AND ADDRESS(ES)	10. SPONSOR/MONITOR'S ACRONYM(S)
	11. SPONSOR/MONITOR'S REPORT NUMBER(S)

12. DISTRIBUTION/AVAILABILITY STATEMENT
Approved for public release; distribution unlimited

13. SUPPLEMENTARY NOTES
code 1 only

14. ABSTRACT
Develop electromagnetic propagation models, that perform equally well over land and sea and in the presence of anomalous propagation conditions for both surface and airborne emitters, for use in operational or engineering propagation assessment systems.

15. SUBJECT TERMS

16. SECURITY CLASSIFICATION OF:			17. LIMITATION OF ABSTRACT	18. NUMBER OF PAGES	19a. NAME OF RESPONSIBLE PERSON
a. REPORT	b. ABSTRACT	c. THIS PAGE			
unclassified	**unclassified**	**unclassified**	**Same as Report (SAR)**	**11**	

emitters to properly estimate capacity for high-bit-rate systems. Due to the nature of the different environmental regimes and their varying effects over tropospheric and earth-to-satellite geometries, this requires modeling efforts for APM and ESPM2, respectively.

For propagation within the troposphere, in order to characterize the propagation channel for a point-to-point (or node-to-node) communications link, the statistical behavior of the signal fading and amplitude characteristics, including time delay, must be determined over the desired bandwidth. This essentially defines the transfer function of the channel. The split-step Fourier parabolic equation (SSPE) algorithm provides the complex amplitude and phase (group delay) of the continuous wave (CW) signal, therefore, by computing the complex signal over a sampled set of frequencies within a desired bandwidth, the transfer function of the propagation channel for that bandwidth can be determined. The impulse response of the channel can then be computed by a fast Fourier transform (FFT) of the transfer function [1,2]. With the transfer function (or equivalently, the impulse response) now properly characterized, we can determine link quality, link capacity (maximum data rate, bandwidth), and availability, of the transmission channel of the communications system.

For frequencies used in satellite communications, the refractive effect of free electrons in the ionosphere is usually ignored. However, the frequency dependence of phase velocity within the ionosphere causes a wave packet to 'spread' in time. This spreading, if severe enough, can produce inter-symbol interference in digital systems, which degrades system performance. This spreading is enhanced for satellites near the horizon due to the increased path length within the ionosphere.

Our approach to including ionospheric effects will be, first, to utilize previous work done in this area in the past. The effects described above are not new and models, either theoretical or empirical, may exist that can be obtained and implemented in ESPM2. Such models estimate the average (over time and space) of the frequency dependent effects described above. If suitable models cannot be identified, we will calculate the frequency dependent effects by integration along the ray path (known) through a suitable ionospheric model. We have standard ionospheric models in-house which can be utilized for this effort. In some ways, though surely hampered by a much slower calculation time, this approach is desirable in that a more complete description of the effects in time and space would be available from the model ionosphere.

WORK COMPLETED

The initial stage of the channel modeling effort for the APM is focused on accurately characterizing the basic parameters that describe the RF channel for a *static* link. Since the APM is based on the SSPE, we are implementing the more efficient Fourier synthesis technique to determine the transfer function. To this end a sensitivity analysis has been performed on fixed point-to-point emitter/receiver geometries to determine the optimum frequency sampling and time window necessary to properly resolve the relative time delay between various ray paths between the transmitter and receiver terminals.

There has also been some communications between the Atmospheric Propagation Branch and the JTRS JPEO Waveforms Division Deputy Product Manager to obtain radio data for some of the KPP JTRS waveforms, however, there may be a limited data set available due to contractor proprietary information.

The ray tracing program developed in previous years was further enhanced by the addition of frequency dependent ionospheric effects on signal delay and polarization. Ionospheric signal delay can be crucial for wide band digital systems for which differential delay with frequency causes distortion of pulse shape and possible inter-symbol interference for pulse sequence coded (CDMA) systems. Polarization rotation can cause significant system signal loss when rotation causes electric field polarization mis-match at the receive antenna. We have also implemented basic digital signal parameters useful for analysis of system performance. Mainly, this consists of the conversion of carrier signal strength to signal-to-noise level to energy/bit/noise spectral density. This is the basic parameter for further system performance analysis. The addition of an ionospheric model to signal strength calculation also required a large re-write of much of the ray analysis code. The absolute time and space dependence of the ionospheric model makes careful specification of the instantaneous coordinate systems necessary.

In the first two years of this effort an atmospheric ray trace capability suitable for use in applications where large propagation angles are possible, i.e. earth-satellite communications, was developed. The initial version, which allowed refractive variations in height only, was modified to include range dependent variations in order to predict the effects of refractive ducting on earth-satellite propagation modes. With the addition of models for rain attenuation, gaseous absorption, and the effects of earth reflections, the new model is now capable of prediction of carrier signal strength in realistic refractive environments for analysis of satellite communication systems [3,4].

In the past year, we have begun to address frequency dependent effects of transmission through the earth's ionosphere. Initially, this has included the effects of the background ionosphere only. In the future, we also hope to include the effects of ionospheric variability, which can play an important role in limiting effective operation of communication systems and also signal intelligence applications, where we hope this tool will find use.

Recognizing that carrier signal strength predictions are of somewhat limited value for digital communication systems, we have also done some work on the addition of basic digital predictive capabilities. Since the range of possibilities in this area is large and we have no specific user supplied direction for this development, we have chosen to focus on the ionospheric effects this year. As the user community for this predictive tool increases, we expect that further digital capabilities will be developed as needed.

RESULTS

Transfer Function

In determining the transfer function, $H(f)$, and subsequent impulse response, $h(t)$, a general approximation must be made for the frequency sampling and bandwidth necessary to properly resolve the multipath components for a given geometry. The general methodology in determining $h(t)$ is straightforward, however, there are many subtle trade-off issues in selecting the optimum parameters to maximize the overall efficiency of the algorithm.

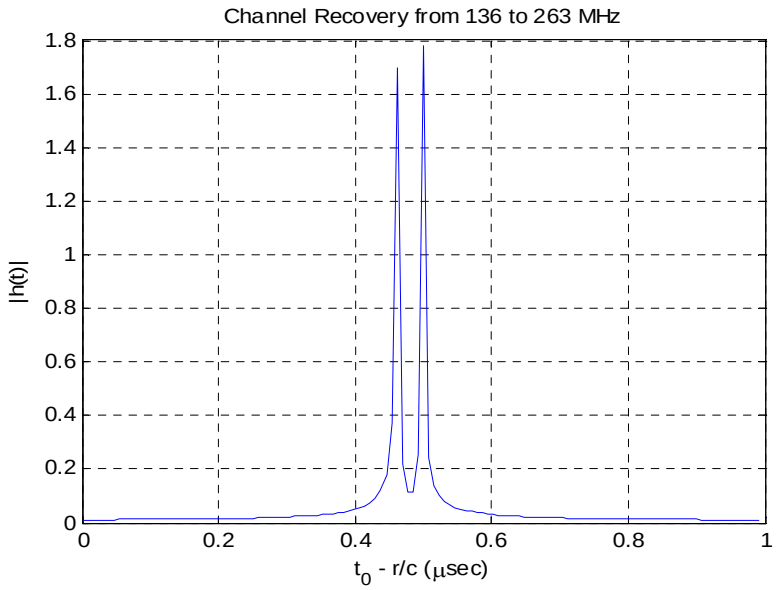

Figure 1. Impulse response for a simple 2-ray path geometry showing the relative time delay difference between the direct and reflected field components.

Figure 1 shows the impulse response computed for a canonical case where the emitter is located 150 m above a smooth sea surface and the receiver is located at a range of 5 km and 200 m in height. For this geometry there are only two field components (direct and reflected) that reach the receiver, and the difference in delay time between the two components can easily be computed via ray trace. Knowing the time delay difference apriori dictates the maximum bandwidth needed in order to sample *H(f)* via the SSPE, and indeed with the proper parameters chosen, the two pulses can be resolved in the time window shown in Fig. 1 by Fourier synthesis.

The FFT size required to determine *h(t)* in Fig. 1 was relatively small at 2^7 (128). The time delay difference for this case is roughly 0.04 microseconds. For longer range propagation paths, particularly in the presence of surface-based ducting, the multipath time delay differences may be fairly small, on the order of nanoseconds. This will necessarily require larger FFT sizes and sampling over larger frequency bandwidths. This will be problematic as the height mesh size, Δz , determined within the SSPE algorithm is a function of wavelength and propagation angle:

$$\Delta z = \frac{\lambda}{2\sin\theta} \,. \tag{1}$$

In order to get both the proper amplitude and phasing from the PE field for a specified geometry, Δz must be consistent across the entire frequency band of interest. This will then dictate the maximum propagation angles required over this band. This is where care must be taken as the SSPE is inherently a small-angle approximation technique. Also, because of the particular implementation of the SSPE within the APM, the particular frequency used also has a "soft" propagation angle limit associated with it due to filtering both in *p*-space (angle space) and *z*-space (i.e., over-filtering will over-attenuate the PE field). Therefore, the modifications necessary to the APM will be more extensive in order to maintain its numerical efficiency. This will be apparent particularly when performing similar computations at HF bands (STANAG, HF ATC, and to some extent SINCGARS) where the wavelength varies from 150 m (2 MHz)

to 10 m (30 MHz), making the variation in the PE propagation angle extremely large in order to maintain consistency in Δz. However, the notion of multipath at HF for short range communications, where the dominant propagation mechanism is the surface wave may not apply and the same SSPE technique for determining the frequency transfer function at VHF and above may not be necessary, or even valid, at HF. We are investigating this further.

The methodology of using Fourier synthesis to determine the impulse response only applies when using the SSPE, and because of the hybridization of the APM, other means of determining *h(t)* in regions where the flat-earth, ray optics, and extended optics techniques are implemented must be developed. Therefore, the methodology to determine *h(t)* under this task will be limited to low altitude geometries.

Ionospheric Delay

Unlike the earth's atmosphere, the free electrons which exist in the ionosphere cause frequency dependent propagation effects on electromagnetic waves. Generally speaking, these effects are most pronounced at lower frequencies. In particular, at typical satellite communication frequencies (900 MHz-tens of GHz), refractive effects are very small and we ignore the ionospheric component in determination of the ray path connecting a ground station to a satellite above or within the ionosphere. The very small signal delay (relative to atmospheric delay) produced in the ionosphere can be important however, especially for multi-user digital communication systems (i.e., CDMA) where timing tolerances become critical.

The frequency dependent propagation delay produced in the ionosphere is given by

$$D = \int_B^T \frac{ds}{v} \ , \tag{2}$$

where *ds* is an element of the ray path in the ionosphere (determined by the homing procedure in the ray trace program), *B,T* are the effective bottom (~50 km) and top of the path in the ionosphere and *v* is the group velocity of the wave in the ionosphere. The group velocity is given by c/n_g, where *c* is the speed of light in vacuum and n_g is the group index-of-refraction in the ionosphere. Under simplifying assumptions valid for the high frequencies in use here, the group index-of-refraction can be approximated by

$$n_g = \frac{1}{n} = \frac{1}{\sqrt{1-\omega_p^2/\omega^2}} \sim 1+\omega_p^2/2\omega^2 \ , \tag{3}$$

where *n* is the phase index-of-refraction, $\omega_p^2 = Ne^2/\varepsilon_o m$ is the square of the angular plasma frequency, *N* is electron density, *e* is electron charge, ε_o is free space permittivity, *m* is electron mass and ω is the angular operational frequency. With these approximations the ionospheric contribution to the total delay time becomes

$$D = \frac{C}{\omega^2}\int_B^T N ds = \frac{C}{\omega^2} TEC \ , \tag{4}$$

where *C* is a constant and *TEC* is the 'Total Electron Content'. It is the integral of the ionospheric electron density, *N*, along the ray path through the ionosphere.

Calculation of the group delay requires a model for the ionospheric electron density and several options were investigated for this effort. In particular, the International Reference Ionosphere (IRI) and the Parameterized Ionospheric Model (PIM) are already used in another model within AREPS and could be used for this effort also. However, these models are relatively slow and the calculation of TEC requires many calculations of *N* along the ray path.

Recognizing the need for a fast, accurate calculation, a model called 'NeQuick' was developed and made available by the ITU [5] for use in TEC calculations. The model is used extensively in the community and its accuracy has proved acceptable, relative to IRI and PIM [6,7]. Inputs to NeQuick consist of a location (sub-latitude, sub-longitude, height), sunspot number, time, and month. Output is a prediction of the electron density at the point for the given conditions. The values of *N* are then integrated along the ray path to produce the required TEC calculation.

In Figure 2 we show the results of ray predictions for a transit of the IRIDIUM 8 satellite in early September of 2008. The ray fan shows the results of ray homing from a transmitter site chosen to lie in Afghanistan, near the Pakistan border, at a set of times (minutes relative to epoch of the TLE) when the satellite was above the horizon as seen from the ground site. The satellite rose at about 1230 local time. The elevations and azimuths listed are those determined from the ray trace program. Note that the satellite rose in the southwest (viewed from the ground site) and set in the northwest. It reached its peak elevation of ~16.5° (relative to the ground site) 6 minutes into the pass, almost due west of the ground site.
In the top left section of Figure 3 we show the calculated propagation delay for each ray shown in Fig.

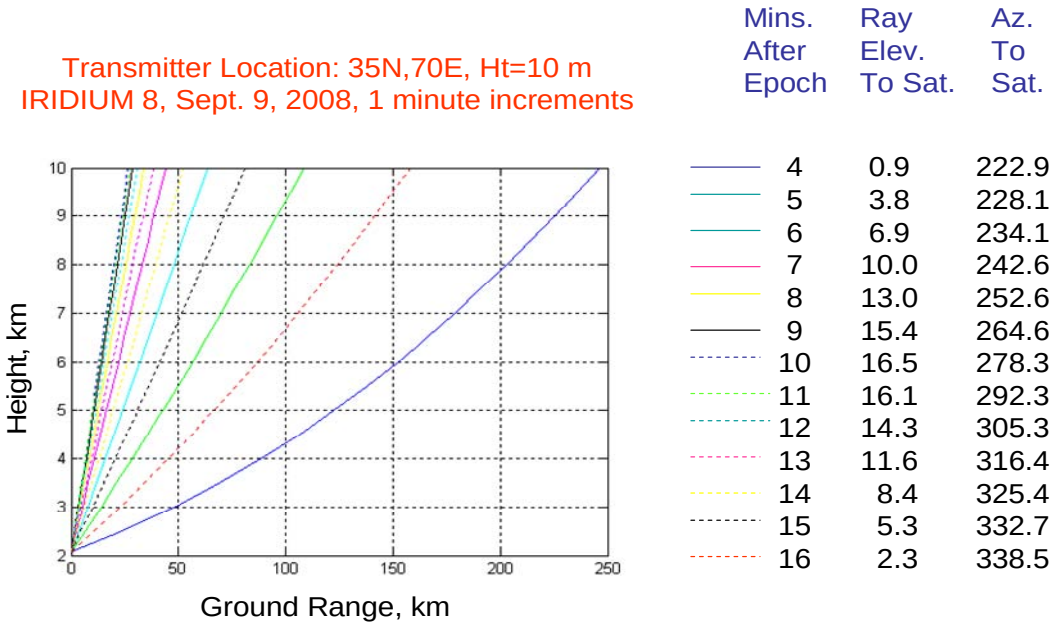

Figure 2. Ray fan in a standard atmosphere from ground transmitter site to IRIDIUM 8 satellite for an orbit in September, 2008. Ray elevations determined by ray trace homing procedure. The satellite locations for each ray change in 1 minute increments and only the bottom 10 km of each ray is shown for display purposes.

2. The atmospheric delay, shown in green in the figure, is simply related to ray path length. For the standard atmosphere used for the ray calculations, the longest ray paths are obtained at the lowest elevation angles, at satellite rise and satellite set. The minimum delay is obtained at maximum elevation, 6 minutes into the pass.

The ionospheric delay, shown in red, is somewhat more complicated as the effect of the TEC is included in the calculation. The maximum ionospheric delay occurs at satellite rise, when the ray path is long and oriented to the southwest (~223 ° azimuth). In this direction the ionosphere has a generally larger electron density causing an increased TEC. In contrast, at satellite set, the orientation is to the northwest (~338° azimuth), and even though the satellite elevation angle (and hence ray length), is similar to the satellite rise ray, for this orientation the ionospheric density is less and the effect of TEC on delay is reduced.

Polarization Rotation

Polarization rotation (Faraday rotation) occurs when an electromagnetic wave propagates in a magnetoplasma, such as the ionosphere. The effect is a rotation of the electric field vector of the wave due to a secondary electric field induced by the motion of free electrons in the plasma as the wave passes. The induced motion of the electrons across the earth's geomagnetic field produces a secondary field in the polarization plane of the generating wave field which, though usually very small in the ionosphere, adds to the field of the wave to produce a total field which is rotated with respect to the initial wave field. As the wave propagates through the magnetoplasma there is a contributing rotation at every point which adds to produce a significant effect. For linear transmit and receive systems the rotation alone can produce up to 3 dB loss. A complete derivation of the equations which govern Faraday rotation is available in most plasma physics texts. Here we present a simplified demonstration based on dimensional analysis which produces the same result as the detailed derivation.

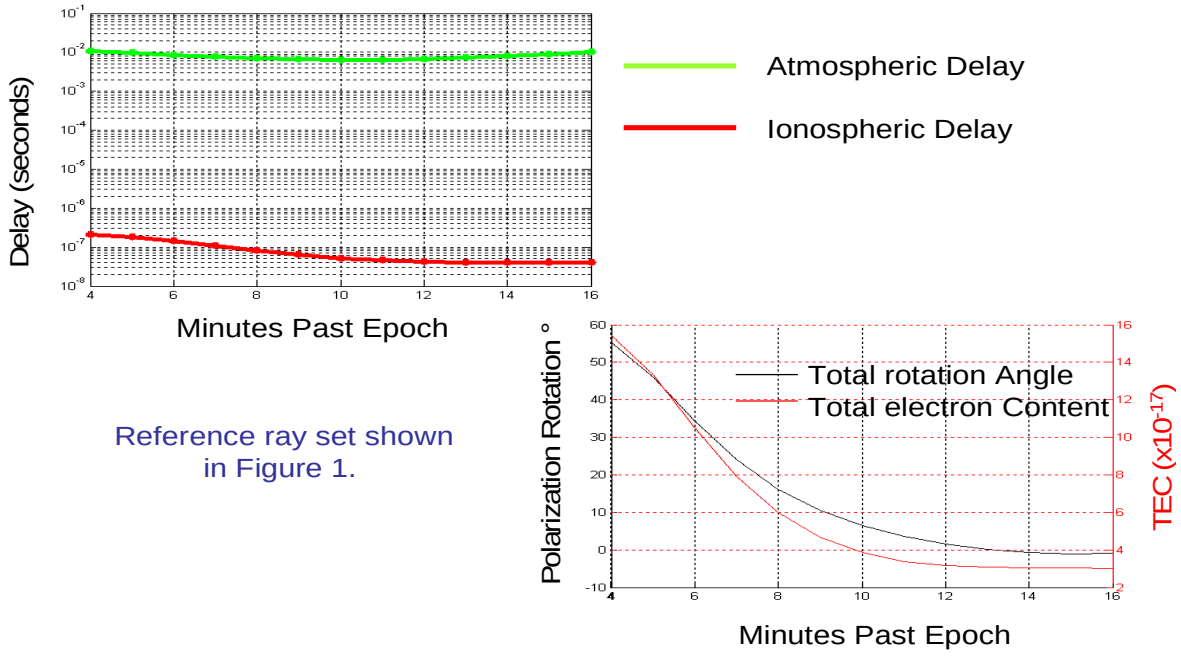

Figure 3. The effect of the ionosphere on total propagation delay (top left) and polarization rotation angle and TEC (bottom right). Plots reference rays in Figure 2.

The electric field of an electromagnetic wave propagating in the ionosphere causes the free electrons in the plasma to rotate around the geomagnetic field. The angular frequency of the rotation, called the gyrofrequency, is given by $\omega_b = eB_f/m$, where e is the charge of an electron, m is mass of an electron and B_f is the component of the geomagnetic field in the direction of the ray path. The rotation of the field over a distance ds can then be written as $\omega_b ds/v_p$ where $v_p = c(1-\omega_p^2/\omega^2)^{1/2}$ is the phase velocity of the wave in the plasma and c is the speed of light in vacuum. Making the same high frequency approximation we used earlier, we obtain the following expression for the total angle of rotation suffered by the wave field in the plasma,

$$\theta = \frac{C_o}{\omega^2} \int_B^T NB_f \, ds \qquad (4)$$

where C_o is a constant and the other parameters were defined earlier. Implementation of the Faraday rotation calculation requires a model for the earth's magnetic field and a model for the ionospheric electron density. For our implementation we use NeQuick for the density model and we have implemented the International Geomagnetic Reference Field [8] for determining the magnetic field. The implementation of the polarization rotation model has also required a major rewrite of much of our computer code since we are required to be more careful in defining our coordinate systems throughout the ray trace model.

Some results of the polarization rotation calculation are shown in Fig. 3, in the bottom right panel. The results refer to the ray fan shown in Fig. 2 as described above. The left vertical axis (black) shows the total rotation of the electric field for each ray in the fan. The right vertical axis (red) shows the TEC for each ray. As we mentioned earlier, at satellite rise the satellite is in the southwest where the electron density is larger. This is reflected in both the TEC and rotation angles for the initial rays. As the satellite continues in its orbit it passes to the northwest where the density is smaller, which is again reflected in both the TEC and total rotation angle.

The calculation of delay and polarization rotation show the effect of the background ionosphere on rays which pass into, or through, the ionosphere. For the IRIDIUM satellite used in the above demonstrations, the satellite is orbiting at about 780 km above the earth. For geostationary satellites the effects of the ionosphere can be much larger as the ray paths pass completely through the ionosphere and traverse the lower latitude ionosphere which, generally, has larger electron densities.

Digital Signal Parameters

We have also done some work on implementation of basic digital communication capabilities this year. As mentioned earlier, we chose to focus on ionospheric effects this year as the type of information applicable for a specific user will have to be provided by potential customers as the model is introduced into the community. Here we provide an example of how the signal strength predictions output by the model can be used to provide performance predictions for digital systems.

Previously, we have discussed and presented examples of the basic signal strength output from the model [3]. Several output formats are possible but for this application, the most useful is the received power, P_r. Received power determined in the model considers transmitter power, transmitter system

losses, transmit antenna directive gain and propagation losses such as free space spreading, rain attenuation and gaseous absorption. We also consider the directive gain of the receive antenna and receive system losses.

Determination of the contribution of all noise sources, both external and internal to the receive system, then allows the signal-to-noise parameter, SN=P_r/N, to be determined. The value for the noise is generally determined in the bandwidth W of the receiver. For simplicity we assume that the transmitted carrier is 100% modulated by the information signal (if not, the received power is reduced by another loss factor). Then we can write $E_b/N_o=(P_r/N)W/R$ where R is the bit rate (bits transmitted per second). The parameter E_b/N_o is the bit energy per noise spectral density and is the basic parameter for digital system performance analysis and is required input for error analysis and system design.

There are many options available to a user with an estimate of E_b/N_o in hand and it can be obtained directly (with a noise determination) from the ray trace model. All these options will make for a wide range of application decision aids designed to satisfy specific requirements for various users/customers that can be developed under 6.4 funding or other transition sponsors.

IMPACT/APPLICATIONS

The goal of this work is to produce operational RF propagation models for incorporation into U.S. Navy assessment systems. Current plans call for the APM to be the single model for all tropospheric radio propagation applications. As APM is developed it will be properly documented for delivery to the OAML, from which it will be available for incorporation into Navy assessment systems. Recent optimizations and enhancements of APM not only benefits the U.S. Navy but also **unifies** the overall military EM performance assessment capability by having a single high-fidelity propagation model that performs equally well over land and sea and in the presence of anomalous propagation conditions.

The primary payoff of this task is providing U.S. Navy and Marine Corps communicators the propagation models necessary for RF digital communications performance assessment for not only JTRS-compliant systems, but all communications systems currently in operational use. With the development of the ESPM2, the Navy and Marine Corps, as well as Army communicators, will also have a propagation model for SATCOM performance assessment to allow optimization of earth-space communications.

TRANSITIONS

All APM modifications and added capabilities transition into the Tactical EM/EO Propagation Models Project (PE 0603207N) under PMW 120 which has produced the Advanced Refractive Effects Prediction System (AREPS). Current and new software, along with information displays will also transition to PMW 120 and/or software projects for inclusion in the Naval Integrated Tactical Environmental Subsystem (NITES) 2 Redesign (N2R). Propagation modeling capabilities can also be transitioned to the Hazardous Weather Detection Display Capability (HWDDC) for use in future refractivity from clutter (RFC) integration plans.

Academia and other U.S. government are also utilizing APM/AREPS. The APM is currently being used by foreign agencies as the underlying propagation model within their own assessment software

packages. The APM has also been adopted as the preferred propagation model in the Ship Air Defence Model (SADM), which is an operational analysis software tool developed to simulate the defense of a naval task group against multiple attacking anti-ship missiles and aircraft. BAE Systems, Australia are the developers of SADM and some of their customers include U.S. DoD agencies.

RELATED PROJECTS

Efforts under this task are related to the JTRS program and the Communication Assets Survey and Mapping (CASM) Tool. CASM is used Nationwide for planning and gap analysis of communications interoperability between state, local and Government agencies. It has been deployed to 77 urban areas across the Nation, and is expanding to statewide use. This tool was used during Operation Golden Phoenix for DoD and first responder communications planning and is currently being investigated for use by the Navy Expeditionary Combat Command, the National Communications System, First Naval Construction Division, and the Naval Coastal Warfare Squadron, as well as other military components in Hawaii and Alaska.

REFERENCES

1. K.H. Craig, M.F. Levy, "Field Strength Forecasting With the Parabolic Equation: Wideband Applications", International Conference on Antennas and Propagation (ICAP 89) Proceedings, 6th, Coventry, England, Apr. 4-7, 1989, p. 461-465.

2. M. Le Palud, "Terrestiral Wireless Channel Modeling", Communications for Network-Centric Operations: Creating the Information Force, MILCOM 2001, Vol. 2, p. 1270-1274, 2001.

3. Sprague, R.A., "Ray-optics- based Signal Strength Prediction Method for the Earth-to-Satellite Propagation Model with Meteorology (ESPM2) in the Advanced Refractive Effects Prediction System, SPAWAR Systems Center", SSC Pacific TD3227 (In press).

4. Sprague, R.A. and P. Babu, "A New Propagation Prediction Tool for Earth-Space Geometries for the Advanced Refractive Effects Prediction System (AREPS)", paper accepted for presentation at MILCOM 2008, Nov. 17-19, 2008, San Diego, CA.

5. ITU RECOMMENDATION R P.531-7 Ionospheric propagation data and prediction methods required for the design of satellite services and systems, 2003.

6. Stankov, S.M., P. Marinov and L. Kutiev, 'Comparison of NeQuick, PIM and TSM model results for the topside ionospheric plasma scale height', , *Advances in Space Physics,* Vol. 39, No. 5, 2007, p. 767-773.

7. Coisson, P, S.M. Radicella, R. Leitinger and B. Nava, 'Topside electron density in IRI and NeQuick: Features and limitations', *Advances in Space Physics,* Vol. 39, No. 5, 2006, pp. 937-942.

8. Macmillan, S. and S. Maus, 'International Geomagnetic Reference Field- the tenth generation', Earth Planet Space, Vol.57, p. 1135-1140, 2005.

PUBLICATIONS

Barrios, A.E., "Modeling Surface Layer Turbulence Effects at Microwave Frequencies", Proc. of IEEE Radar Conference, RADARCON 2008, 26-30 May 2008, Rome, Italy.

Sprague, R.A., "Ray-optics- based Signal Strength Prediction Method for the Earth-to-Satellite Propagation Model with Meteorology (ESPM2) in the Advanced Refractive Effects Prediction System, SPAWAR Systems Center", SSC Pacific TD3227 (In press).

Sprague, R.A., P. Babu, "A New Propagation Prediction Tool for Earth-Space Geometries for the Advanced Refractive Effects Prediction System (AREPS)", *Joint IEEE Ant. & Prop. / URSI Symposium*, July 5-12, 2008, San Diego, CA.

Sprague, R.A. and P. Babu, "A New Propagation Prediction Tool for Earth-Space Geometries for the Advanced Refractive Effects Prediction System (AREPS)", paper accepted for presentation at MILCOM 2008, Nov. 17-19, 2008, San Diego, CA.